Cumulative Absolute Velocity (CAV) and Seismic Intensity Based on the PEER-NGA Database

Kenneth W. Campbell,[a] **M.EERI and Yousef Bozorgnia,**[b] **M.EERI**

Cumulative absolute velocity (CAV) has been proposed as an instrumental index to quantify the potential earthquake damage to structures. We explore this idea further by developing a relationship between the standardized version of CAV and the Japan Meteorological Agency (JMA) and modified Mercalli (MMI) instrumental seismic intensities in order to correlate standardized CAV with the qualitative descriptions of damage in the corresponding macroseismic intensity scales. Such an analysis statistically identifies the threshold values of standardized CAV associated with the onset of damage to buildings of good design and construction inherent in these scales. Based on these results, we suggest that CAV might be used to rapidly assess the potential damage to a general class of conventional structures after an earthquake. However, other ground motion or damage-related parameters might be better suited to quantifying the potential damage to structures of a specific type and size. [DOI: 10.1193/1.4000012]

INTRODUCTION

In 1988, the Electric Power Research Institute (EPRI) introduced cumulative absolute velocity (CAV) as a potential damage-related ground motion intensity measure (IM). CAV is mathematically defined by the equation (EPRI 1988, Reed and Kassawara 1990):

$$\mathrm{CAV} = \int_0^{t_{max}} |a(t)|dt \tag{1}$$

where $|a(t)|$ is the absolute value of acceleration at time t and t_{max} is the total duration of the ground motion record. In 1991, EPRI introduced a standardized version of CAV, which we refer to as $\mathrm{CAV_{STD}}$ in order to distinguish it from the original definition of CAV, that prevents low-amplitude, nondamaging ground motions from contributing to the value of CAV. $\mathrm{CAV_{STD}}$ is mathematically defined by the equation (EPRI 2006):

$$\mathrm{CAV_{STD}} = \sum_{i=1}^{N} \left(H(PGA_i - 0.025) \int_{i-1}^{i} |a(t)|dt \right) \tag{2}$$

[a] EQECAT, Inc., 1030 NW 161st Place, Beaverton, OR 97006-6337; kcampbell@eqecat.com
[b] PEER, 325 Davis Hall, University of California, Berkeley, CA 94720-1792; yousef@berkeley.edu

Earthquake Spectra, Volume 28, No. 2, pages 457–485, May 2012;

where N is the number of nonoverlapping one-second time intervals, PGA_i is the peak ground acceleration (g) in time interval i (inclusive of the first and last points), and $H(x)$ is the Heaviside step function given by the equation:

$$H(x) = \begin{cases} 0 & x < 0 \\ 1 & x \geq 0 \end{cases} \tag{3}$$

EPRI (1991) provided a different mathematical expression for CAV_{STD} that gives identical results. Figure 1 shows a hypothetical acceleration record and the corresponding values of CAV and CAV_{STD} as they evolve over time. According to Equations 1 and 2, CAV and CAV_{STD} are the values obtained at the end of the record. As this figure shows, CAV_{STD} will always be equal to or less than CAV. This difference can be quite large for long-duration small-amplitude records.

Since their introduction, CAV, CAV_{STD}, and several other proposed versions of CAV have been extensively studied for use as potential damage-related IMs (Campbell and Bozorgnia 2010a, 2010b, 2011b). Most of these studies have correlated these IMs with instrumental or macroseismic intensities and, by inference, to the qualitative levels of structural damage that are inferred from these intensities. A few studies have gone a step further and related these IMs directly to observed damage or to the computed nonlinear structural response of model buildings.

A panel of industry, government, and regulatory experts convened by EPRI (EPRI 1988, Reed and Kassawara 1990) was the first to evaluate CAV as a potential damage-related IM.

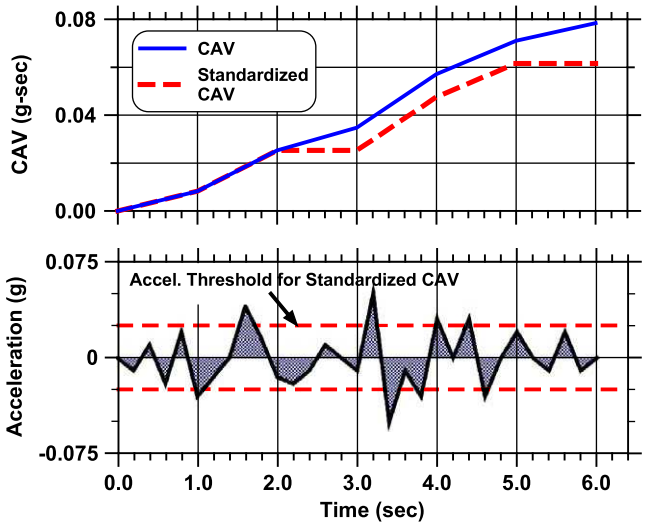

Figure 1. Illustration of the definitions of CAV and standardized CAV (CAV_{STD}) showing their evolution with time. The hypothetical acceleration time series is that given in EPRI (1991). The acceleration threshold for determining when the value of CAV_{STD} in any nonoverlapping one-second interval is included in the summation is 0.025 g. Modified from EPRI (1991).

In a preliminary study, the panel used 39 records considered to be of engineering significance to evaluate a number of ground motion, duration, and elastic and inelastic structural response parameters, including CAV and Arias intensity (AI; Arias 1970), for their ability to adequately quantify damage. The following steps were performed in the investigation of each of these parameters:

1. Compute the parameter value for each earthquake record.
2. Pair each computed parameter value with the corresponding observed MMI for the station at which the record was obtained.
3. Find the record with the lowest parameter value (this value is the parameter threshold) for which the intensity is greater than MMI VI (i.e., MMI equal to VII).
4. Count the number of earthquake records with MMI VI or less which have parameter values above the threshold (these records represent those cases for which the parameter would erroneously, but conservatively, predict potential damage to buildings of good design and construction.

The results of this initial investigation indicated that the following IMs should be pursued further: AI (unfiltered and filtered above 10 Hz), CAV (unfiltered and filtered), peak ground acceleration (PGA) (unfiltered and filtered), 5%-damped pseudo-absolute response spectral acceleration (PSA) (unfiltered), and the average PSA over the frequency range 2–10 Hz (unfiltered). The panel included PGA because of its widespread use and not because of its strong relationship to damage. The panel selected MMI VII as the threshold intensity of potentially damaging ground motion for "*buildings of good design and construction*," based on the qualitative description of damage in the MMI scale (Richter 1958, EPRI 1988, USGS 2000). Buildings of good design and construction, a term taken from the U.S. Geological Survey version of the MMI scale, are defined as "buildings which have reasonable earthquake protection, but have not necessarily been designed by an engineer (e.g., block and brick walls reinforced with steel and wood-framed houses which are anchored to their foundations)" (USGS 2000).

In order to confirm the preliminary results and to strengthen the bases for the threshold values, the panel expanded the database to 263 recordings and repeated the analyses. The panel found that CAV (unfiltered and filtered) was the most "discriminating parameter" with the fewest number of erroneous records (20 and 19, respectively) of MMI VI or less that exceeded the threshold. AI (filtered) was next with 33 erroneous records, followed closely by AI (unfiltered) with 39 erroneous records. For reference, PGA had 156 erroneous records. The damage threshold values determined by the panel for some key ground motion parameters were 0.318 and 0.319 g-s for unfiltered and filtered CAV, 12.6 and 11.2 cm/s (after multiplying by $\pi/2g$ and converting from g^2-s units) for unfiltered and filtered AI, 0.253 g for the largest value of PSA in the frequency range 0–10 Hz, and 0.200 g for the average value of PSA in the frequency range 2–10 Hz. The panel also performed a study that directly correlated CAV with damage data. This study is described in a later section.

Based on the engineering characteristics of ground motion and the investigations of earthquake records and associated damage summarized in EPRI (1988) and Reed and Kassawara (1990), the panel recommended the following two-level criterion for determining when an

earthquake has exceeded the operating basis earthquake ground motion (OBE) at a nuclear power plant (i.e., when the ground motion is expected to be potentially damaging to conventional buildings of good design and construction):

1. Response Spectrum Check: The 5%-damped PSA at the site, at frequencies between 2 and 10 Hz, exceeds the corresponding OBE design response spectrum or 0.20 g, whichever is greater
2. CAV Check: The CAV value is greater than 0.30 g-s

Only the 0.20 g threshold for PSA is relevant for the general application of the above two-level criterion to conventional buildings of good design and construction applied in this study. EPRI (1991) later recommended that CAV should be replaced by CAV_{STD} in the above damage criterion and recommended that the threshold for the potential onset of damage for CAV_{STD} should be decreased to 0.16 g-s, based on the same analyses that were used to determine the original CAV threshold.

Since it was first defined, there have been many studies that have proposed the use of CAV or one of its variants as an instrumental index to account for duration in the characterization of ground motion or to quantify earthquake damage to conventional and nuclear structures from such ground motions. The USNRC (1997) formally adopted a slightly revised version of the recommendations in EPRI (1988, 1991) to assess the potential for a ground motion record to cause damage to a nuclear facility. The U.S. Nuclear Regulatory Commission (USNRC) proposed the use of CAV_{STD} (the *CAV check*) and the response spectrum (the *response spectrum check*) in its post-event procedures to determine whether the OBE response spectrum is exceeded and the nuclear power plant must be shut down for inspection after an earthquake. However, unlike EPRI, the response spectrum check was further subdivided into a *spectral acceleration (PSA) check* and a *spectral velocity (PSV) check*. A more detailed description of these checks are given in USNRC (1997) and in Campbell and Bozorgnia (2010a, 2011b).

Cabañas et al. (1997) used 25 recordings from four earthquakes in Italy (M_L 4.7, 5.0, 5.1, 6.1) to test several relationships between representative parameters of ground motion energy and damage data. They observed that two of these parameters, AI and CAV_{STD}, showed good correlation with the macroseismic effects observed in the earthquakes. Based on this preliminary analysis, they further evaluated unfiltered and band-pass filtered versions of AI and several versions of CAV_{STD} with values of threshold acceleration (PGA_i) that ranged from 5 to 25 cm/s^2. They correlated these IMs with locally determined Medvedev-Sponheuer-Karnik (MSK) intensity and observed damage and found that the best correlation was for unfiltered AI and for the version of CAV_{STD} with $PGA_i = 0.02$ g, nearly the same as the 0.025 g threshold proposed by EPRI (1991). They found, however, that none of these IMs correlated well with observed structural damage, except for buildings of the poorest construction type (e.g., buildings constructed of field stone, adobe, etc.).

Kramer and Mitchell (2006) used 450 ground motion records from 22 earthquakes in active tectonic regimes in an attempt to find a single IM to use in the evaluation of soil liquefaction. Approximately 300 candidate IMs were investigated that reflected various aspects of the amplitude, frequency content, and duration of earthquake ground motion. A series of soil profiles were analyzed to evaluate the different IMs. For each analysis,

an input motion was applied at the base of the soil profile and the resulting response of the profile was computed, neglecting the effects of pore pressure redistribution. They found that a version of CAV that excludes all of those acceleration pulses (not just those in one-second intervals) with accelerations less than 5 cm/s^2 (0.005 g) was the best IM to relate to the generation of excess porewater pressure in potentially liquefiable soils. They refer to this IM as CAV_5. They also developed a ground motion prediction equation (GMPE) for CAV_5 in order to demonstrate its predictability.

Tselentis and Danciu (2008) developed relationships between observed MMI and the common logarithms of PGA, peak ground velocity (PGV), AI, and CAV using 310 records from 89 earthquakes in the Greek strong-motion database. In order to reduce the observed biases in the residuals, they found that they needed to include magnitude, distance, and site conditions as independent variables in the relationships. Their final MMI relationships had standard deviations of 0.666 (PGA), 0.661 (PGV), 0.649 (AI), and 0.679 (CAV), indicating that all four IMs were equally good at predicting MMI when the physical parameters of the earthquake and site were also included in the relationships.

Danciu (personal communication) repeated the analysis described by EPRI (1988) and Reed and Kassawara (1990) using the 310 records in the Greek strong-motion database using a number of peak-amplitude, response spectral, and damage-related IMs. He determined that CAV_5, with a threshold value (the smallest value for those sites with MMI VII or greater) of 83 cm/s (0.085 g-s), was the most "discriminating parameter" with the fewest number of erroneous records of MMI VI or less that exceeded this threshold. The top five performers (and their corresponding number of erroneous components) were CAV_5 (39), CAV_{10} (42), CAV_{15} (46), AI (53), and CAV (59), where the subscripts refer to the limit (in cm/s^2) above which an acceleration pulse is included in the CAV calculation. He also developed fragility curves in terms of CAV_5 for 3-, 6-, and 12-story model reinforced-concrete structures designed to the European building code and found that there was less than a 10% probability that these structures would suffer minor damage at the CAV_5 threshold value.

GMPEs have been developed for several variants of CAV including the original definition of CAV (Danciu and Tselentis 2007, Campbell and Bozorgnia 2010a, 2010b), CAV_{STD} (Kostov 2005, EPRI 2006), CAV_5 (Kramer and Mitchell 2006), and CAV_{DP} (Campbell and Bozorgnia 2010a, 2011b). The parameter CAV_{DP} is a version of CAV_{STD} that incorporates the two-level damage threshold criterion of EPRI as adapted for use by the USNRC. It is described in more detail below. The GMPEs of EPRI (2006) and Campbell and Bozorgnia (2010a, 2011b) relate CAV_{STD} to PGA and CAV, respectively, which requires that a GMPE be used to predict these latter IMs when they are unknown (e.g., when used in a seismic hazard analysis). Kostov (2005) developed his GMPE using the European strong-motion database. Kramer and Mitchell (2006) and EPRI (2006) developed their GMPEs using subsets of an early version of the database developed as part of the Pacific Earthquake Engineering Research Center (PEER) Next Generation Attenuation (NGA) Project (Power et al. 2008). Danciu and Tselentis (2007) developed their GMPE from the Greek strong-motion database. Campbell and Bozorgnia (2010a, 2010b, 2011b) used a subset of the final PEER-NGA database (Chiou et al. 2008) to develop their GMPEs with the expressed purpose of (1) determining the overall level of predictability and reliability of CAV and CAV_{DP} and (2) comparing their GMPEs with those that they developed using the same database for

peak ground motion and elastic response spectral parameters (Campbell and Bozorgnia 2008), inelastic response spectral parameters (Bozorgnia et al. 2010), and the Japan Meteorological Agency (JMA) instrumental seismic intensity (Campbell and Bozorgnia 2010a, 2011a).

All of the above studies found that some version of CAV is as good as or is superior to other peak-amplitude, response spectral, duration-based, and damage-related IMs, based on their correlation with seismic intensity or observed damage and their high level of predictability (i.e., their relatively small standard deviations). Although AI was found to be a close second to the CAV-related parameters, we exclude it from further consideration because of its significantly larger standard deviation (Danciu and Tselentis 2007, Campbell and Bozorgnia 2010b, 2011c). We selected CAV_{DP} as the CAV-related IM to statistically evaluate in this study because of its direct relationship to the damage threshold criterion recommended by EPRI (1988, 1991) and Reed and Kassawara (1990) for buildings of good design and construction and its adoption by the USNRC to conservatively indicate the potential damage to nuclear facilities. We acknowledge that other versions of CAV, or even other IMs, might correlate well or better than CAV_{DP} with structural damage to buildings of a specific type and size (e.g., Akkar and Özen 2005), but our objective in this study is to show the feasibility of using a single damage-related IM to represent the damage potential of ground motion to a general class of structures rather than to a specific structure.

CAV_{DP} is mathematically defined by the expression (Campbell and Bozorgnia 2011b):

$$CAV_{DP} = \begin{cases} CAV_{STD}; & \text{if the PSA and CAV checks are exceeded} \\ CAV_{STD}; & \text{if the PSV and CAV checks are exceeded} \\ 0; & \text{otherwise} \end{cases} \tag{4}$$

in which the PSA, PSV, and CAV checks are exceeded when all of the following criteria are met:

$$\max(\max[PSA_{H1}(2-10\text{ Hz})],\ \max[PSA_{H2}(2-10\text{ Hz})],\ \max[PSA_{V}(2-10\text{ Hz})]) > 0.20\text{ g} \tag{5}$$

$$\max(\max[PSV_{H1}(1-2\text{ Hz})],\ \max[PSV_{H2}(1-2\text{ Hz})],\ \max[PSV_{V}(1-2\text{ Hz})]) > 15.34\text{ cm/s} \tag{6}$$

$$\max([CAV_{STD}]_{H1},\ [CAV_{STD}]_{H2},\ [CAV_{STD}]_{V}) > 0.16\text{ g-s} \tag{7}$$

where $H1$ and $H2$ refer to the first and second horizontal components of the acceleration record, V refers to the vertical component, and the terms $\max[PSA_X(2\text{–}10\text{ Hz})]$ and $\max[PSV_X(1-2\text{ Hz})]$ represent the maximum values of the 5%-damped PSA and PSV within the respective frequency ranges indicated in parentheses. We also evaluate the original version of CAV_{DP} recommended by EPRI (1991) that excludes the PSV check in order to show the sensitivity of the results to this check.

There have been no subsequent studies, other than those by the authors (Campbell and Bozorgnia 2010a), that have statistically quantified the basis for the damage threshold

criterion proposed by EPRI (1988) and revised by EPRI (1991) for buildings of good design and construction. In order to provide a statistical basis for this parameter, we developed a prediction equation between CAV_{DP} and the geometric mean horizontal component of CAV (Campbell and Bozorgnia 2011b), which we refer to as CAV_{GM}. When the value of CAV_{GM} is unknown, which will usually be the case when conducting a seismic hazard analysis, it can be predicted from a GMPE such as that developed by Campbell and Bozorgnia (2010b) but with a subsequent increase in aleatory uncertainty. Although such a GMPE shows how CAV depends on the physical parameters of an earthquake, it does not provide an independent assessment of the statistical significance and potential conservatism that is associated with the EPRI and USNRC damage threshold criteria embodied in their definitions of CAV_{DP}. A comprehensive evaluation of the conservatism in these criteria would require the type of engineering studies that EPRI (1988, 1991) originally performed to develop these criteria, which is beyond the scope of this study. However, some insight into the potential degree of conservatism implied by these criteria can be gained by determining the statistical correlation between CAV_{DP} and seismic intensity. In this study, we present such a statistical correlation by developing simple prediction equations between CAV_{DP} and instrumental measures of both JMA seismic intensity and MMI and using these relationships to correlate CAV_{DP} to the qualitative degrees of damage described in the corresponding JMA and MMI macroseismic scales. We also correlate CAV_{DP} with the recently developed European macroseismic scale (EMS), based on the latter scale's close relationship to MMI (Musson et al. 2010). This latter scale is often referred to as EMS-98.

RELATIONSHIP BETWEEN SEISMIC INTENSITY AND DAMAGE

Macroseismic intensity is typically determined subjectively from observations of the effects of an earthquake on humans, man-made structures, and the natural environment (e.g., Musson et al. 2010). However, the proliferation in the number of strong-motion instruments over the last few decades and the need for a quick assessment of damage after an earthquake has spawned the development of instrumental measures of the JMA and MMI seismic intensity scales. In this section, we summarize the qualitative descriptions of damage inferred in the JMA, MMI, and EMS macroseismic intensity scales and relate these descriptions to the potential damage threshold criteria for CAV proposed by EPRI and USNRC, based on the strong correlation between the macroseismic and instrumental measures of these intensity scales.

JMA INTENSITY

The JMA macroseismic intensity scale (also known as the *shindo* scale) has been used in Japan as a measure of earthquake ground shaking effects since 1949. Traditionally, JMA intensity was subjectively assigned to one of seven categories. In 1996, the scale was revised to ten categories and each category was defined in terms of an instrumental parameter, which was calibrated to coincide with the effects described in the macroseismic version of the scale (JMA 1996, Earthquake Research Committee 1998). This instrumental seismic intensity is calculated from either ground motion acceleration records or specially designed seismic intensity meters. We refer to this new instrumental seismic intensity measure as I_{JMA} (Campbell and Bozorgnia 2011a). It should be noted that, since 1996, JMA seismic intensities are calculated and are *not* determined from the observed phenomena described in the

macroseismic scale. Therefore, although I_{JMA} was originally calibrated to this scale, the macroseismic effects at a site will not necessarily be consistent with the assigned seismic intensity.

I_{JMA} is computed from the Fourier amplitude spectrum of the ground acceleration record in several steps: (1) the Fourier transform of each of the three components of the record (i.e., two horizontal and one vertical) is calculated for a selected time window, (2) a band-pass filter is applied to these Fourier transforms in the frequency domain, (3) the inverse Fourier transforms of the filtered Fourier spectra are calculated, (4) the absolute value of the geometric mean of the three transformed times series is computed at each time increment and the total duration (τ) of those pulses that exceed acceleration values ranging from zero to the maximum of the record are calculated, and (5) the acceleration value a_0 (cm/s^2) having a total duration τ_0 satisfying the condition $\tau(a_0) \geq 0.3$ s is defined from which I_{JMA} is calculated by the equation:

$$I_{JMA} = 2.0 \log a_0 + 0.94 \tag{8}$$

The algorithms for calculating I_{JMA} are described in greater detail by Sokolov and Furumura (2008) and Campbell and Bozorgnia (2010a, 2011a). These latter authors summarize several of the recent GMPEs that have been developed for I_{JMA} and discuss several studies that correlate I_{JMA} with MMI and other strong-motion IMs.

The revised ten-degree JMA macroseismic intensity scale is described in terms of the effects of an earthquake on humans, indoor and outdoor objects, wooden houses, reinforced-concrete (RC) structures, ground and slopes, utilities and infrastructure, and large-scale structures (JMA 2011). For purposes of this study, we have chosen to use the qualitative effects of an earthquake on RC structures as described in this seismic intensity scale to demonstrate the correlation of I_{JMA} with damage. These effects, along with the ranges of I_{JMA} that correspond to each JMA macroseismic intensity category, are summarized in Table 1. Qualitative levels of damage in Table 1 are given for RC structures of both high and low earthquake resistance. According to this table, there is no visible damage (i.e., formation of cracks) to RC structures of low earthquake resistance at JMA 5 Lower (5L), corresponding to $4.5 \leq I_{JMA} < 5.0$, and to RC structures of high earthquake resistance at JMA 5 Upper (5U), corresponding to $5.0 \leq I_{JMA} < 5.5$. According to the online table, earthquake resistance tends to be higher for newer buildings. It is generally considered to be low for Japanese structures built prior to 1982 and high for structures built after this date, based on a major revision of the Japanese building code at that time. However, earthquake resistance is not dependent only on the age of the building.

MODIFIED MERCALLI INTENSITY

Since its development in 1931 (Wood and Neumann 1931) and revision in 1956 (Richter 1958), there has been a long history of studies that have correlated MMI to strong-motion IMs, mostly for the purpose of estimating PGA, PGV, and PSA for engineering evaluation and design. A few of the more widely used older studies are described in Campbell (1986). More recently, Wald et al. (1999b) developed relationships between PGA, PGV, and MMI in California for use in an application that rapidly generates an instrumental intensity map after an earthquake, which they refer to as ShakeMap

Table 1. The relationship between JMA seismic intensity and the effects of an earthquake on reinforced-concrete (RC) structures

JMA Seismic Intensity		Level of Earthquake Resistance	
Macroseismic	Instrumental	High	Low
5 Lower (5L)	$4.5 \leq I_{JMA} < 5.0$	No damage	No damage
5 Upper (5U)	$5.0 \leq I_{JMA} < 5.5$	No damage	Cracks may form in walls, crossbeams and pillars.
6 Lower (6L)	$5.5 \leq I_{JMA} < 6.0$	Cracks may form in walls, crossbeams and pillars.	Cracks are more likely to form in walls, crossbeams and pillars.
6 Upper (6U)	$6.0 \leq I_{JMA} < 6.5$	Cracks are more likely to form in walls, crossbeams and pillars.	Slippage and X-shaped cracks may be seen in walls, crossbeams and pillars. Pillars at ground level or on intermediate floors may disintegrate, and buildings may collapse.
7	$I_{JMA} \geq 6.5$	Cracks are even more likely to form in walls, crossbeams and pillars. Ground level or intermediate floors may sustain significant damage. Buildings may lean in some cases.	Slippage and X-shaped cracks are more likely to be seen in walls, crossbeams and pillars. Pillars at ground level or on intermediate floors are more likely to disintegrate, and buildings are more likely to collapse.

(Wald et al. 1999c). Other recent relationships between peak ground motion and response spectral parameters and MMI or similar intensity scales have been developed by Atkinson and Sonley (2000), Ebel and Wald (2003), Davenport (2003), Atkinson and Kaka (2007), Tselentis and Danciu (2008), and Faenza and Michelini (2010). Sokolov and Chernov (1998) and Sokolov (2002) developed relationships between Fourier amplitude spectra and MMI. Because of the well-defined correlation between I_{JMA} and the qualitative description of damage to RC structures given in Table 1, it is useful to correlate I_{JMA} with MMI, or more specifically, to an instrumental measure of this intensity, which we refer to as I_{MM}. We are aware of two such relationships developed by Shabestari and Yamazaki (2001) and Sokolov and Furumura (2008).

Shabestari and Yamazaki (2001) derived the following relationship between I_{MM} and the instrumental value of a_0 (cm/s^2) used to calculate I_{JMA}:

$$I_{MM} = 3.93 \log a_0 - 1.17 \tag{9}$$

which has a standard deviation of 0.274 and a coefficient of determination (R^2 value) of 0.989. This relationship is based on the correlation of the geometric mean of a_0 for a specified MMI category with USGS assessments of MMI (converted to an integer value) at 105 recording sites of the 1987 Whittier Narrows (**M** 6.0), 1989 Loma Prieta (**M** 6.9),

and 1994 Northridge (**M** 6.7), California, earthquakes. They used this equation together with Equation 8 to develop a relationship between I_{MM} and I_{JMA} given by the equation:

$$I_{MM} = 1.95\, I_{JMA} - 2.91 \tag{10}$$

which has a standard deviation of 0.283 and a R^2 value of 0.987. This relationship is considered to be valid for instrumental intensities in the range $3.5 \le I_{MM} \le 8.5$ and $3.5 \le I_{JMA} \le 6.0$. According to this equation, the median values of I_{MM} that are consistent with the threshold values of JMA intensity for which visible damage (i.e., the formation of cracks) to RC structures of low earthquake resistance is seen (JMA 5U or $I_{JMA} = 5.0$) is $I_{MM} = 6.84 \pm 0.28$ or MMI VII, and for which visible damage to RC structures of high earthquake resistance is seen (JMA 6L or $I_{JMA} = 5.5$) is $I_{MM} = 7.82 \pm 0.28$ or MMI VIII. Shabestari and Yamazaki show that their relationship between I_{MM} and MMI is consistent with similar relationships between MMI and both community Internet intensity (CII) (Dengler and Dewey 1998, Wald et al. 1999a) and peak-amplitude measures of I_{MM} estimated from PGA and PGV (Wald et al. 1999b), the latter of which are used in the development of USGS ShakeMaps (Wald et al. 1999c).

Sokolov and Furumura (2008) developed a relationship between I_{MM} and I_{JMA} using 598 acceleration records from nine Japanese earthquakes of JMA magnitude 6.3 to 8.0 that occurred between 1999 and 2007. The records came from the K-Net and KiK-Net strong-motion networks that were deployed throughout Japan by the National Institute for Earth Science and Disaster Research (NIED) following the destructive 1995 Kobe, Japan, earthquake (Aoi et al. 2004). I_{MM} was calculated using the Fourier amplitude spectra (FAS) method of Sokolov (2002) and I_{JMA} was calculated from Equation 8. The relationship is given by the equation:

$$I_{MM} = 1.743\, I_{JMA} - 0.584 \tag{11}$$

which has a standard deviation of 0.384 and a R^2 value of 0.984. The relationship is considered to be valid for instrumental intensities in the range $5.5 \le I_{MM} \le 10.5$ and $3.5 \le I_{JMA} \le 6.0$. According to this equation, the median values of I_{MM} that are consistent with the threshold values of JMA intensity for which visible damage to RC structures of low earthquake resistance is seen (JMA 5U or $I_{JMA} = 5.0$) is $I_{MM} = 8.13 \pm 0.38$ or MMI VIII, and for which visible damage to RC structures of high earthquake resistance is seen (JMA 6L or $I_{JMA} = 5.5$) is $I_{MM} = 9.00 \pm 0.38$ or MMI IX.

The large difference between the estimates of I_{MM} given by Equations 10 and 11 would at first appear to potentially limit our ability to reliably assign a specific value of I_{MM} to a given JMA intensity level. Sokolov and Wald (2002) found a similar discrepancy between the FAS method of Sokolov (2002) and the peak-amplitude method of Wald et al. (1999b) from a direct comparison of calculated I_{MM} values from the 1999 (**M** 7.1) Hector Mine, California, and 1999 (**M** 7.6) Chi-Chi, Taiwan, earthquakes. They found that the peak-amplitude method produced I_{MM} values that were approximately one intensity unit lower than Equation 11, which is more consistent with the estimates from Equation 10. Sokolov and Wald (2002) suggest that the FAS method, which is based on worldwide data and, therefore, averages different building codes and qualities of construction, provides a worst-case or pessimistic

assessment of I_{MM} and that the peak-amplitude method, which reflects improved building practices, provides a more current or optimistic view. These authors go on to say that the peak-amplitude relationships of Wald et al. (1999b) also estimate lower intensity levels for the same peak motions than the relationship of Trifunac and Brady (1975), which was based on older MMI assessments similar to those used by Sokolov (2002). They further suggest that the shift between the old and new generation of intensity correlations may be related to improved building practices in the United States. Thus, insofar as the peak-amplitude method is based primarily on data from recent earthquakes in California, it characterizes existing building stock constructed in accordance with the more modern building codes. Wald et al. (1999b) also note that their relationship uses a more restricted intensity range than that of Trifunac and Brady (1975), which screens out the less reliable recordings. In addition, the USGS practice of assigning MMI from field observations has shifted from one of assigning the highest observed macroseismic intensity to assigning more of an average or predominant intensity at a given location (Dewey et al. 1995).

Because of the demonstrated bias in the predicted intensities from Equation 11 and the demonstrated consistency of the predicted intensities from Equation 10 with: (1) modern qualitative assessments of MMI determined by the USGS, (2) instrumentally calculated estimates of MMI used to develop ShakeMaps, and (3) MMI derived from CII assessments, we adopted this latter relationship to develop the correlation between the MMI and JMA macroseismic intensity scales given in Table 2. In this table, the range in I_{MM} values that correspond to the given range in I_{JMA} are shifted approximately 0.3 intensity units higher than the range that corresponds to the assigned MMI category. We believe that this shift is acceptable considering that it is about equal to the standard deviation in the estimate of I_{MM} and that the majority of the range falls within the assigned MMI category. Furthermore, the relationship between the JMA and MMI intensity categories given in Table 2 is generally consistent with that given by Musson et al. (2010).

One drawback of the MMI scale is that it gives only a very general qualitative description of damage, which is biased toward masonry structures (Richter 1958). According to the USGS (2000), there are four classes of structures: (1) specially designed structures (Masonry A), (2) buildings of good design and construction (Masonry B), (3) ordinary substantial structures (Masonry C), and (4) poorly built structures (Masonry D). The assignment of a USGS structure class to a specified masonry type (Richter 1958, EPRI 1988) is that of the authors

Table 2. The relationship between instrumental and macroseismic measures of MMI and JMA seismic intensity

I_{JMA}	JMA Macroseismic Intensity	I_{MM}	Modified Mercalli Macroseismic Intensity
$4.5 \le I_{JMA} < 5.0$	5 Lower (5L)	$5.87 \le I_{MM} < 6.84$	VI
$5.0 \le I_{JMA} < 5.5$	5 Upper (5U)	$6.84 \le I_{MM} < 7.82$	VII
$5.5 \le I_{JMA} < 6.0$	6 Lower (6L)	$7.82 \le I_{MM} < 8.79$	VIII
$6.0 \le I_{JMA} < 6.5$	6 Upper (6U)	$8.79 \le I_{MM} < 9.77$	IX
$I_{JMA} \ge 6.5$	7	$I_{MM} \ge 9.77$	X

and not that of the USGS. The USGS describes the degree of damage as negligible, slight, and considerable. Fortunately, this shortcoming has been addressed in the recently developed EMS scale described in the next section. For this study, we use the more detailed descriptions of damage to RC structures in the EMS scale to describe the damage inferred by the same intensity category in the MMI scale, based on a study by Musson et al. (2010) that found that the two scales (as well as the Mercalli-Cancani-Sieberg scale, or MCS scale, and the MSK-64 scale described in the next section) are generally equivalent to one another up to at least intensity X. It should be noted that the direct correspondence among these intensity scales was not necessarily true in previous comparisons (e.g., Richter 1958).

EUROPEAN MACROSEISMIC INTENSITY

The EMS-98 scale (or simply EMS scale) is an update of the MSK scale, which itself is an update based on experiences available in the early 1960s from the application of the MCS scale commonly used in Italy, the MMI scale commonly used in the United States, and the Medvedev (GEOFIAN) scale commonly used in Russia and countries of the former Soviet Union (Grünthal 1998). Moderate changes to the MSK scale were proposed by Medvedev in 1976 and 1978. At that time, it became evident that the scale needed several improvements, including more clarity and an adjustment to incorporate more modern construction techniques. These improvements were eventually implemented in the EMS scale.

The EMS scale was specifically designed to describe the damage to structures of different construction types and vulnerability classes (Grünthal 1998). Continuing with our example, RC structures fall into the EMS structure type described as RC frames and walls with levels of earthquake-resistant design (ERD) described as none, moderate, or high. Each of these levels of earthquake resistance is assigned a range of vulnerability classes from A to F with the higher letters corresponding to the less vulnerable and more earthquake-resistant structures. In order to account for uncertainty, each level of earthquake resistance is assigned a most likely vulnerability class as well as less likely stronger and weaker vulnerability classes. Vulnerability Class F represents the strongest of those RC frames and walls that are described as having a high level of earthquake resistance. We refer to this vulnerability class as having a very high level of earthquake resistance and consider it to correspond to the vulnerability associated with the most rugged of structures, such as safety related nuclear structures and other critical structures located in high seismic areas.

According to the qualitative descriptions of damage to RC structures in the EMS scale (Tables 3 and 4), the onset of slight structural damage (Damage Grade 2) to structures of Vulnerability Class C (no specific ERD) begins at EMS VII and increases by one degree of intensity for each increase in vulnerability class (Grünthal 1998). For example, the onset of structural damage to Vulnerability Class F (very high ERD), described as cracks in columns and beams, begins at EMS X. This is generally consistent with the JMA intensity scale for which the onset of damage to RC structures of low earthquake resistance, which is assumed to be similar to EMS Vulnerability Class C (no specific ERD), begins at JMA 5U, and for which the onset of damage to RC structures of high earthquake resistance, which is conservatively assumed to be similar to EMS Vulnerability Class D (moderate ERD), begins at JMA 6L. According to Table 2, these JMA intensities correspond to EMS/MMI VII and VIII, respectively.

Table 3. The relationship between EMS macroseismic intensity and the effects of an earthquake on reinforced-concrete (RC) frames and walls

	Level of Earthquake Resistance and Most Likely Vulnerability Class			
EMS Intensity	Very High* (Class F)	High (Class E)	Moderate (Class D)	None (Class C)
V	No damage	No damage	No damage	No damage
VI	No damage	No damage	No damage	A few buildings sustain damage of Grade 1†.
VII	No damage	No damage	A few buildings sustain damage of Grade 1.	A few buildings sustain damage of Grade 2.
VIII	No damage	No damage	A few buildings sustain damage of Grade 2.	Many buildings sustain damage of Grade 2; a few of Grade 3.
IX	No damage	A few buildings sustain damage of Grade 2.	Many buildings sustain damage of Grade 2; a few of Grade 3.	Many buildings sustain damage of Grade 3; a few of Grade 4.
X	A few buildings sustain damage of Grade 2.	Many buildings sustain damage of Grade 2; a few of Grade 3.	Many buildings sustain damage of Grade 3; a few of Grade 4.	Many buildings sustain damage of Grade 4; a few of Grade 5.

*Very high is the term we give to less likely, highly earthquake-resistant Class F structures.
†See Table 4 for a description of damage grades.

Table 4. EMS classification of damage to reinforced-concrete (RC) frames and walls

Damage Grade	Structural Damage	Nonstructural Damage	Description
1	None	Slight	Fine cracks in plaster over frame members or in walls at the base; fine cracks in partitions and infills.
2	Slight	Moderate	Cracks in columns and beams of frames and in structural walls; cracks in partition and infill walls; fall of brittle cladding and plaster; falling mortar from the joints of wall panels.
3	Moderate	Heavy	Cracks in columns and beam column joints of frames at the base and at joints of walls; spalling of concrete cover; buckling of reinforced rods; large cracks in partition and infill walls; failure of individual infill panels.
4	Heavy	Very heavy	Large cracks in structural elements with compression failure of concrete and fracture of rebars; bond failure of beam reinforced bars; tilting of columns; collapse of a few columns or of a single upper floor.
5	Very Heavy	–	Collapse of ground floor or parts (e.g., wings) of buildings.

EPRI DAMAGE REVIEW

The expert panel convened by EPRI (1988) reviewed 263 strong-motion records for which there were observed or estimated values of MMI and well-documented damage to buildings and structures in the vicinity of the site. The panel grouped the intensity data into three damage data categories defined as follows: 0, industrial or power facilities with engineered structures and equipment; 1, buildings of good design and construction that were not necessarily designed by an engineer; and 2, situations where an adequate description of damage was not available for determining which damage data category to use, but where the panel was able to state whether the earthquakes and ground motions were potentially damaging to buildings of good design and construction. The panel suggested that the type of conventional building construction defined by Data Categories 1 and 2 is a conservative surrogate for the seismic capacity of nuclear power facilities, but noted that conventional buildings and structures consistent with Data Category 0 were the closest in design and construction to these facilities.

The EPRI panel found that the onset of damage associated with Data Category 0 begins at MMI VIII and that the onset of damage associated with Data Categories 1 and 2 begins at MMI VII. This agrees with the USGS version of the MMI scale (USGS 2000), which states that the onset of damage to buildings of good design and construction (Data Categories 1 and 2) begins at MMI VII, and to specially designed structures, assumed to be consistent with Data Category 0, at MMI VIII. The panel's assessment is also generally consistent with the EMS scale (Table 3), which states that the onset of structural damage to RC frames and walls of Vulnerability Class C (no specific ERD), assumed to be consistent with Data Categories 1 and 2, begins at EMS VII, and to RC frames and walls of Vulnerability Class D (moderate ERD), assumed to be consistent with Data Category 0, at EMS VIII. We believe that the panel's assessment is also generally consistent with the JMA intensity scale (Table 1), which describes the onset of damage to RC structures with low earthquake resistance, which is assumed to be consistent with Data Categories 2 and 3, as starting at JMA 5U (EMS/MMI VII according to Table 2), and to RC structures with high earthquake resistance, which is assumed to be consistent with Data Category 0, as starting at JMA 6L (EMS/MMI VIII according to Table 2). Therefore, all of the macroseismic intensity scales reviewed in this paper appear to be consistent with the panel's conclusion regarding the level of intensity at which the onset of damage occurs in conventional buildings of good design and construction and in engineered industrial and conventional power facilities (i.e., specially designed structures according to the MMI scale).

The EPRI panel also reviewed the available earthquake experience data for equipment at conventional power plants and heavy industrial facilities and found that it supported the conclusion that there is "reasonable engineering assurance that equipment at nuclear power plants will not fail at intensities less than MMI VIII," (EPRI 1988, p. 4-53). This is consistent with the panel's conclusion regarding the onset of structural damage to these same types of facilities. After reviewing all of the damage data at its disposal, the panel concluded that assuming the potential for damage to nuclear power facility equipment and structures occurs at MMI VII, consistent with that of conventional buildings of good design and construction, is sufficiently conservative to determine whether there is damage to nuclear power facilities.

Based on the direct correlation of the original CAV damage threshold criterion with actual damage data, EPRI (1988) determined that ground motions that cause damage to buildings of good design and construction are a factor of at least 1.5 times larger than the originally

recommended threshold value of 0.30 g-s. Using these same data, EPRI (1991) determined that the revised threshold value of 0.16 g-s associated with CAV_{STD} is a factor of five lower than the lowest value associated with documented damage to conventional industrial and power facilities, or 0.8 g-s, and a factor of three lower than the lowest value associated with documented damage to buildings of good design and construction, or 0.5 g-s. These assessments further confirm the conservatism implied by the EPRI and USNRC damage threshold criteria.

PREDICTION EQUATIONS

The purpose of developing relationships between CAV_{DP} and the instrumental intensity measures I_{JMA} and I_{MM} is twofold: (1) to evaluate the values of I_{JMA} and I_{MM} that correspond to the CAV_{DP} damage threshold criterion of 0.16 g-s representing the potential onset of damage to (a) buildings of good design and construction as described in the MMI intensity scale, no specific earthquake-resistant design as described in the EMS intensity scale, and low earthquake resistance as described in the JMA intensity scale and (b) the shutdown of a nuclear power plant when the OBE has been exceeded, and (2) to statistically correlate CAV_{DP} with the qualitative descriptions of damage to RC structures and other buildings of good design and construction that are described in the JMA, MMI, and EMS macroseismic intensity scales.

DATABASE

The strong-motion database used in this study was developed by PEER for use in the NGA-West Project (Power et al. 2008, Chiou et al. 2008). To show the sensitivity of the results to the database selection criteria, we also used the subset of the PEER-NGA database that we previously used to develop GMPEs for peak ground motion and linear elastic response spectral parameters (Campbell and Bozorgnia 2007, 2008), inelastic response spectral parameters (Bozorgnia et al. 2010), CAV_{GM} (Campbell and Bozorgnia 2010b), I_{JMA} (Campbell and Bozorgnia 2011a), and CAV_{DP} (Campbell and Bozorgnia 2011b). It is referred to in this paper as the CB08-NGA database and is described in detail by Campbell and Bozorgnia (2007, 2008).

The definition of CAV_{DP} given in Equation 4 embodies all of the EPRI (1988, 1991) and USNRC (1997) damage threshold criteria within a single IM. However, we note that EPRI did not include the PSV check in its original recommendations, which was later added by the USNRC in the formulation of its nuclear power plant shutdown criteria. Campbell and Bozorgnia (2010b) performed an analysis of the CB08-NGA and PEER-NGA databases and found that inclusion of the PSV check allows ground motions at relatively long distances from large-magnitude earthquakes to initiate plant shutdown when the PSA and CAV checks would not (see also Figure 2). Such ground motions are generally not of concern if the primary use of CAV_{DP} is to screen out near-source high-acceleration records from small-magnitude earthquakes, which was EPRI's original intent when defining the response spectrum check. Nevertheless, in order to demonstrate the impact of including the PSV check in the definition of CAV_{DP}, and to potentially broaden the applicability of CAV_{DP} as a potential damage index parameter, we provide results with and without this check. In the remainder of the paper, we refer to these databases as CB08-NGA-PSV, CB08-NGA-NoPSV, PEER-NGA-PSV, and PEER-NGA-NoPSV, where the terms PSV and NoPSV refer to whether the PSV check is applied when selecting the records. These databases are summarized in Table 5 and in Figure 2.

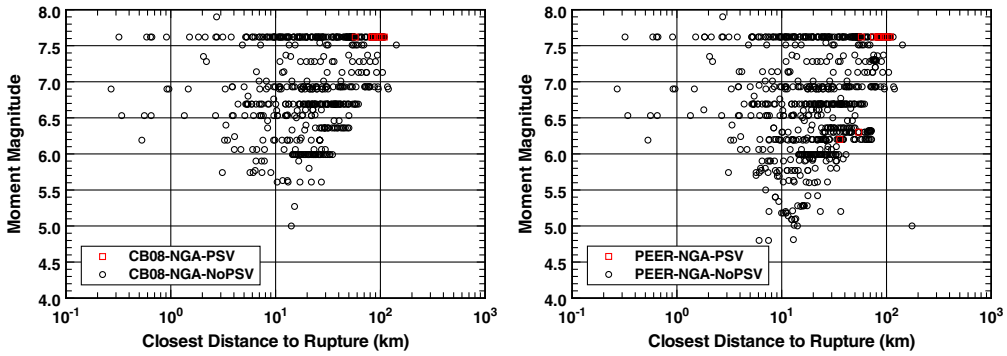

Figure 2. Distribution of records with respect to moment magnitude (M) and distance (R_{RUP}): (left) CB08-NGA databases, (right) PEER-NGA databases. The red squares are those additional records that exceed the PSV check.

MEDIAN MODEL

The median relationship between CAV_{DP} and instrumental seismic intensity is given by the equation:

$$\mu_{\ln CAV_{DP}} = c_0 + c_1 X \tag{12}$$

where $\mu_{\ln CAV_{DP}}$ is the predicted median value of $\ln CAV_{DP}$ (g-s) and X is either I_{JMA} or I_{MM}. Analyses were performed using the random-effects regression algorithms of Abrahamson and Youngs (1992). These relationships are restricted to intensities in the range $I_{JMA} \geq 4.5$ and

Table 5. Summary of strong-motion databases used in the development of the prediction equations

Database	PSV Check	No. of Events	No. of Records		M	R_{RUP} (km)
			No.	Percentage*		
JMA Instrumental Intensity ($I_{JMA} \geq 4.5$)						
CB08-NGA-PSV	Yes	45	558	36.2%	5.0–7.9	0.1–142
CB08-NGA-NoPSV	No	45	550	35.7%	5.0–7.9	0.1–142
PEER-NGA-PSV	Yes	94	774	22.2%	4.8–7.9	0.1–176
PEER-NGA-NoPSV	No	94	763	21.9%	4.8–7.9	0.1–176
MMI Instrumental Intensity ($I_{MM} \geq 5.5$)						
CB08-NGA-PSV	Yes	48	675	43.8%	4.9–7.9	0.1–170
CB08-NGA-NoPSV	No	48	650	42.2%	4.9–7.9	0.1–161
PEER-NGA-PSV	Yes	104	944	27.1%	4.8–7.9	0.1–176
PEER-NGA-NoPSV	No	104	914	26.2%	4.8–7.9	0.1–176

*Percentage of the total number of available records.

Table 6. Summary of regression results

Database	PSV Check	c_0	c_1	$\sigma_{\ln CAV_{DP}}$	$\tau_{\ln CAV_{DP}}$	σ_T	R^2
JMA Instrumental Intensity ($I_{JMA} \geq 4.5$)							
CB08-NGA-PSV	Yes	–5.207	0.943	0.329	0.279	0.431	0.657
CB08-NGA-NoPSV	No	–5.165	0.935	0.329	0.281	0.433	0.648
PEER-NGA-PSV	Yes	–5.527	0.987	0.346	0.294	0.454	0.699
PEER-NGA-NoPSV	No	–5.484	0.979	0.348	0.295	0.456	0.692
MMI Instrumental Intensity ($I_{MM} \geq 5.5$)							
CB08-NGA-PSV	Yes	–3.859	0.493	0.295	0.302	0.422	0.740
CB08-NGA-NoPSV	No	–3.829	0.489	0.296	0.306	0.426	0.725
PEER-NGA-PSV	Yes	–4.034	0.505	0.309	0.316	0.442	0.768
PEER-NGA-NoPSV	No	–4.024	0.504	0.311	0.318	0.445	0.759

Note: Predicted value of CAV_{DP} has units of g-s; standard deviations are in natural log units.

$I_{MM} \geq 5.5$ for reasons explained in the next section. The results of the analyses are listed in Table 6 and plots of the equations are shown in Figure 3. We also tested bilinear and quadratic functional forms of the above equation, but hypothesis tests indicated that the additional coefficients were not significantly different from zero at the 90% confidence level.

ALEATORY UNCERTAINTY

Aleatory uncertainty is modeled by the random-effects equation (Abrahamson and Youngs 1992, Campbell and Bozorgnia 2008):

$$\ln CAV_{DP,ij} = \mu_{\ln CAV_{DP},ij} + \eta_i + \varepsilon_{ij} \tag{13}$$

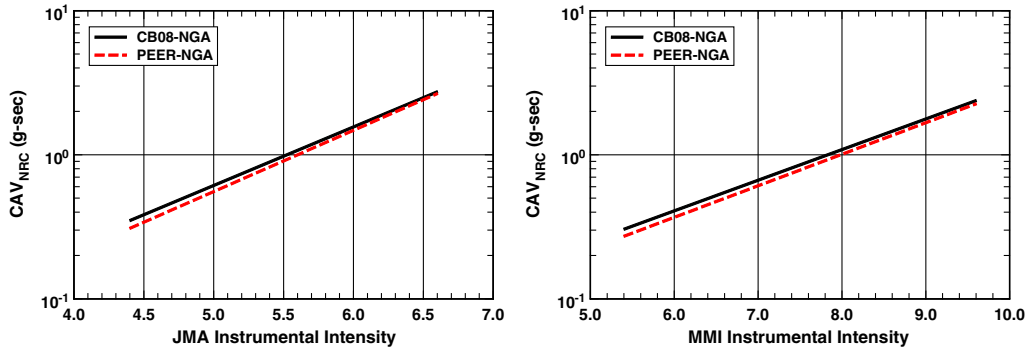

Figure 3. Prediction equations between CAV_{DP} and the instrumental intensity measures I_{JMA} and I_{MM}: (solid line) CB08-NGA databases, (dashed line) PEER-NGA databases. The relationships derived from data that exceed the PSV check are virtually indistinguishable (within the thickness of the lines) from those derived from data that do not exceed this check.

where η_i is the interevent (between-earthquake) residual for event i and the parameters $\mu_{\ln CAV_{DP},ij}$, $\ln CAV_{DP,ij}$, and ε_{ij} are the predicted median value, observed value, and intra-event (within-earthquake) residual for recording j of event i. The independent normally distributed variables η_i and ε_{ij} have zero means and estimated interevent, intra-event, and total standard deviations of $\tau_{\ln CAV_{DP}}$, $\sigma_{\ln CAV_{DP}}$, and $\sigma_T = \sqrt{\tau^2_{\ln CAV_{DP}} + \sigma^2_{\ln CAV_{DP}}}$ (Table 6).

ANALYSIS OF RESIDUALS

An initial regression analysis using all of the data indicated that there was a bias in the residuals for $I_{JMA} < 4.5$ and $I_{MM} < 5.5$ due to the filtering effects of the PSA and CAV_{STD} thresholds used to define CAV_{DP}. As a result, we restricted the analysis to those records with $I_{JMA} \geq 4.5$ and $I_{MM} \geq 5.5$. This does not impact any of the conclusions of our study, since no damage is expected to RC structures classified as having low earthquake resistance at JMA 5L ($I_{JMA} < 5.0$) or as having no specific earthquake-resistant design at EMS/MMI VI ($I_{MM} < 6.5$). Figure 4 shows the distributions of the total residuals with respect to I_{JMA}. The lack of any visible biases or trends in these plots further justifies our use of a linear relationship between I_{JMA} and $\ln CAV_{DP}$. The same results were found for the distributions of residuals with respect to I_{MM} (not shown). There are, however, notable biases and trends between the residuals and the physical parameters of the earthquakes for both intensity measures. Figure 5 shows the distributions of the interevent and intra-event residuals of the I_{JMA} relationship with respect to **M**, R_{RUP}, the median value of rock PGA (A_{1100}) as estimated from the GMPE of Campbell and Bozorgnia (2008), the time-averaged shear-wave velocity in the top 30 m of a site (V_{S30}) and related NEHRP site classes (BSSC 2009), and the depth of sediments beneath the site ($Z_{2.5}$) for the prediction equation based on the CB08-NGA-PSV database. The magnitude bias in the interevent residuals indicates that CAV_{DP} is overestimated at small magnitudes and underestimated at large magnitudes by about 25%. There is no similar trend in the intra-event residuals. Figure 5 also indicates that there are biases in the intra-event residuals at moderate-to-large distances, small-to-moderate rock accelerations, and firm-to-hard rock sites (NEHRP Site Classes A and B). These biases are caused by differences in the way

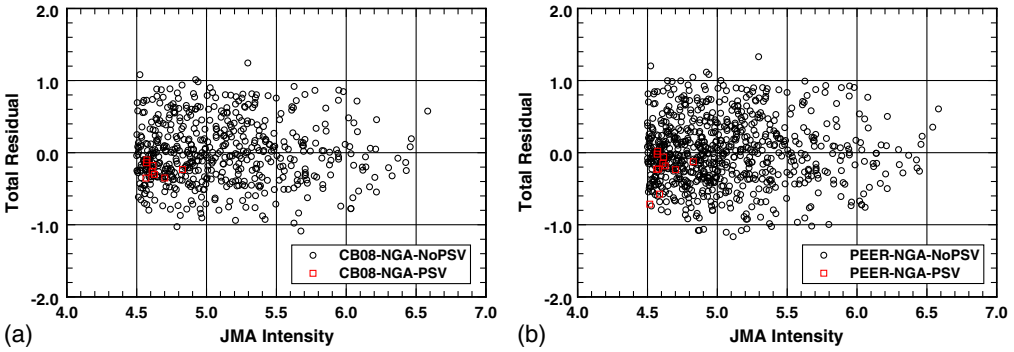

Figure 4. Total residuals for the prediction equations between CAV_{DP} and I_{JMA}: (a) CB08-NGA databases, (b) PEER-NGA databases. The red squares are those additional records that exceed the PSV check.

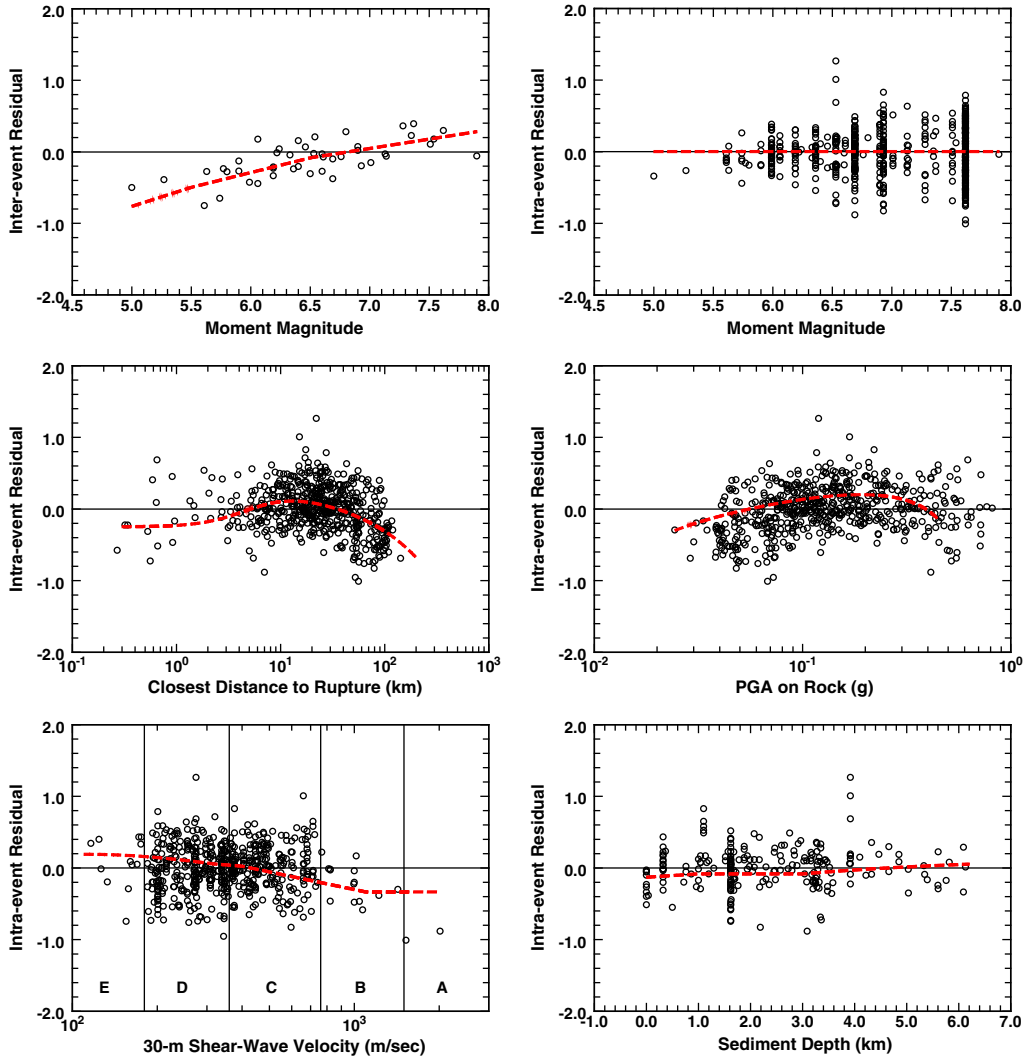

Figure 5. Distribution of interevent residuals with respect to moment magnitude (M) and intra-event residuals with respect to M, rupture distance (R_{RUP}), median PGA on rock (A_{1100}), 30-m shear wave velocity (V_{S30}) binned by NEHRP Site Class, and sediment depth ($Z_{2.5}$). The residuals are calculated from the prediction equation based on the CB08-NGA-PSV database. The dashed lines are the bias predicted from the GMPEs of CAV_{DP} and I_{JMA} developed by Campbell and Bozorgnia (2011a, 2011b) with CAV_{DP} estimated using the median value of CAV_{GM} predicted from the GMPE of Campbell and Bozorgnia (2010b).

that CAV_{DP} and I_{JMA} scale with the physical parameters of the earthquakes. Similar results were found for I_{MM} and the other three databases. We found negligible biases (not shown) in the interevent residuals of rake angle (λ), dip of the rupture plane (δ), and depth to the top of the rupture plane (Z_{TOP}), and in the intra-event residuals of the hanging-wall factor (f_{hng}).

Whether the biases noted in Figure 5 are important depends on the potential use of the prediction equations. Likely uses of these equations are to statistically evaluate CAV_{DP} as a tentative criterion for: (1) initiating an automatic or operator-assisted emergency shutdown of a nuclear reactor (SCRAM) and (2) rapidly assessing whether conventional (i.e., non-nuclear) structures might have sustained damage after an earthquake. In both cases, the physical parameters of an earthquake might not be known with any reliability at the time these criteria are applied, which precludes us from incorporating physical earthquake parameters in Equation 12. As demonstrated in the interevent and intra-event residual plots in Figure 5, if an unbiased relationship between CAV_{DP} and I_{JMA} is desired, one can be obtained from the GMPEs of these IMs (Campbell and Bozorgnia 2010b, 2011a, 2011b). The dashed lines on these plots are the biases estimated by comparing the median predictions of CAV_{DP} and I_{JMA} from these GMPEs with the median predictions of CAV_{DP} from Equation 12, using the median predicted values of I_{JMA} from the same GMPE (i.e., both estimates of CAV_{DP} use the same value of I_{JMA}). There is no available GMPE for I_{MM} (one is currently under development), but we would expect similar results to those found for I_{JMA} considering the common dependence of I_{JMA} and I_{MM} on a_0.

CORRELATION OF CAV_{DP} WITH DAMAGE

In Table 7, we present the statistical correlation of CAV_{DP} with qualitative descriptions of damage to generic RC structures, and by analogy to other buildings of good design and

Table 7. Statistical correlation between CAV_{DP} and JMA macroseismic intensity assuming the onset of damage to buildings of good design and construction begins at $I_{JMA} = 5.0$

JMA	EMS/ MMI	NGA Database	PSV Check	Median (g-s)	σ_T	$P_{ne}(0.16)$	CAV_{DP} (g-s) P_{ne}=5%	P_{ne}=1%	$P_{ne}(0.16)_{5U}$
5U	VII	CB08	Yes	0.611	0.431	9.34×10^{-4}	0.301	0.224	0.160
5U	VII	CB08	No	0.613	0.433	9.65×10^{-4}	0.301	0.224	0.160
6L	VIII	CB08	Yes	0.980	0.431	1.31×10^{-5}	0.482	0.359	0.256
6L	VIII	CB08	No	0.978	0.433	1.46×10^{-5}	0.480	0.357	0.255
6U	IX	CB08	Yes	1.570	0.431	5.84×10^{-8}	0.773	0.576	0.411
6U	IX	CB08	No	1.560	0.433	7.20×10^{-8}	0.766	0.570	0.408
7	X	CB08	Yes	2.516	0.431	8.17×10^{-11}	1.238	0.923	0.658
7	X	CB08	No	2.491	0.433	1.15×10^{-10}	1.222	0.910	0.650
5U	VII	PEER	Yes	0.553	0.418	3.14×10^{-3}	0.262	0.192	0.160
5U	VII	PEER	No	0.555	0.425	3.19×10^{-3}	0.262	0.192	0.160
6L	VIII	PEER	Yes	0.906	0.418	6.68×10^{-5}	0.429	0.315	0.262
6L	VIII	PEER	No	0.905	0.425	7.72×10^{-5}	0.428	0.313	0.261
6U	IX	PEER	Yes	1.484	0.418	4.63×10^{-7}	0.703	0.516	0.429
6U	IX	PEER	No	1.477	0.425	5.47×10^{-7}	0.698	0.511	0.426
7	X	PEER	Yes	2.431	0.418	1.03×10^{-9}	1.152	0.846	0.703
7	X	PEER	No	2.410	0.425	1.36×10^{-9}	1.138	0.834	0.695

Note: Standard deviations are in natural log units; $P_{ne}(0.16)$ is the probability that $CAV_{DP} < 0.16$ g-s given the specified median value of I_{JMA}; $P_{ne}(0.16)_{5U}$ is the nonexceedance probability corresponding to the lower boundary of JMA intensity category 5U (i.e., $I_{JMA} = 5.0$).

construction, by relating estimates of CAV_{DP} with values of I_{JMA} and JMA macroseismic intensity from Tables 1 and 2. This analysis assumes that damage to such structures begins at JMA 5U ($I_{JMA} = 5.0$). Table 8 gives similar results by relating estimates of CAV_{DP} with values of I_{MM} and EMS/MMI macroseismic intensity from Tables 2 and 3, assuming that damage begins at EMS/MMI VII ($I_{MM} = 6.5$). In these tables, $P_{ne}(0.16)$ is the probability that $CAV_{DP} < 0.16$ g-s (the EPRI damage threshold criterion) given the specified median estimate of I_{JMA} or I_{MM}. This probability is an indication of the likelihood that CAV_{DP} will be less than that required to exceed the recommended EPRI damage threshold criteria given the potential level of damage indicated by the macroseismic intensity levels. Also listed in these tables are the predicted values of CAV_{DP} that correspond to nonexceedance probabilities of 1%, 5%, and the value of $P_{ne}(0.16)$ that corresponds to JMA 5U and EMS/MMI VII. It should be noted that the probabilities given in Tables 7 and 8 only account for the aleatory uncertainty associated with the empirical prediction of CAV_{DP} and do not account for the epistemic uncertainty associated with the relationships between macroseismic intensity and damage or between instrumental and macroseismic intensity. Some insight into this epistemic uncertainty can be gained by comparing the results listed in these tables as summarized in the next section.

Table 8. Statistical correlation between CAV_{DP} and EMS/MMI macroseismic intensity assuming the onset of damage to buildings of good design and construction begins at $I_{MM} = 6.5$

JMA	EMS/ MMI	NGA Database	PSV Check	Median (g-s)	σ_T	$P_{ne}(0.16)$	CAV_{DP} (g-s) P_{ne}=5%	P_{ne}=1%	$P_{ne}(0.16)_{VII}$
5U	VII	CB08	Yes	0.520	0.422	2.62×10^{-3}	0.260	0.195	0.160
5U	VII	CB08	No	0.522	0.426	2.76×10^{-3}	0.259	0.194	0.160
6L	VIII	CB08	Yes	0.851	0.422	3.75×10^{-5}	0.425	0.319	0.262
6L	VIII	CB08	No	0.851	0.426	4.38×10^{-5}	0.422	0.316	0.261
6U	IX	CB08	Yes	1.393	0.422	1.46×10^{-7}	0.696	0.522	0.429
6U	IX	CB08	No	1.387	0.426	1.98×10^{-7}	0.689	0.515	0.425
7	X	CB08	Yes	2.281	0.422	1.52×10^{-10}	1.139	0.855	0.702
7	X	CB08	No	2.263	0.426	2.51×10^{-10}	1.123	0.840	0.694
5U	VII	PEER	Yes	0.473	0.442	7.09×10^{-3}	0.229	0.169	0.160
5U	VII	PEER	No	0.473	0.445	7.40×10^{-3}	0.228	0.168	0.160
6L	VIII	PEER	Yes	0.784	0.442	1.62×10^{-4}	0.379	0.280	0.265
6L	VIII	PEER	No	0.783	0.445	1.79×10^{-4}	0.377	0.278	0.265
6U	IX	PEER	Yes	1.299	0.442	1.08×10^{-6}	0.628	0.465	0.439
6U	IX	PEER	No	1.297	0.445	1.29×10^{-6}	0.624	0.461	0.438
7	X	PEER	Yes	2.152	0.442	2.05×10^{-9}	1.040	0.770	0.728
7	X	PEER	No	2.147	0.445	2.69×10^{-9}	1.033	0.762	0.726

Note: Standard deviations are in natural log units; $P_{ne}(0.16)$ is the probability that $CAV_{DP} < 0.16$ g-s given the specified median value of I_{MM}; $P_{ne}(0.16)_{VII}$ is the nonexceedance probability corresponding to the lower boundary of EMS/MMI intensity category VII (i.e., $I_{MM} = 6.5$).

DISCUSSION OF RESULTS

Depending on the database, the probabilities that CAV_{DP} is less than 0.16 g-s [$P_{ne}(0.16)$], given the onset of damage consistent with macroseismic intensities of JMA 5U and EMS/MMI VII and their assumed relationship to I_{JMA} and I_{MM}, are found to range from (rounding to a single significant digit) 0.1–0.3% for the relationship based on I_{JMA} (Table 7) and 0.3–0.7% for the relationship based on I_{MM} (Table 8). These probabilities are calculated based on the threshold values of instrumental intensities that correspond to the lower end of the ranges of values that define intensity categories JMA 5U (i.e., $I_{JMA} = 5.0$) and EMS/MMI VII (i.e., $I_{MM} = 6.5$). This is consistent with how EPRI (1988, 1991) originally selected the CAV and CAV_{STD} damage threshold values and confirms that these threshold values are appropriately conservative for buildings of good design and construction. The values of $P_{ne}(0.16)$ decrease to less than 0.02% for an assumed onset of damage consistent with JMA 6L (i.e., $I_{JMA} = 5.5$) or EMS/MMI VIII ($I_{MM} = 7.5$), which generally corresponds to the onset of damage to industrial and conventional power facilities (EPRI 1988), specially designed structures (MMI scale), and structures with levels of earthquake-resistant design described as moderate (EMS scale) or high (JMA scale).

Although the values of $P_{ne}(0.16)$ estimated in this study are very small, it is beyond the scope of this paper to recommend whether the values of PSA, PSV, and CAV_{STD} conservatively used to define the onset of damage to buildings of good design and construction (EPRI) and to determine when a nuclear power plant must be shut down for inspection after an earthquake (USNRC) can be increased for specific types and classes of structures and equipment. This would require a comprehensive engineering study. However, our results, summarized in Table 9, can be used to provide some insight into the values of CAV_{DP} that are

Table 9. Threshold values of CAV_{DP} and their epistemic uncertainty below which structures of various levels of earthquake-resistant design are not expected to be damaged

Level of Earthquake-Resistant Design			Seismic Intensity		CAV_{DP} (g-s)			
MMI	EMS	JMA	EMS/MMI	JMA	Median	P_{ne}=5%	P_{ne}=1%	$P_{ne}(0.16)_{5U,VII}$
Good Design & Construction	None	Low	VII	5U	0.54 ± 0.05	0.26 ± 0.03	0.19 ± 0.02	0.16 ± 0.00
Specially Designed	Moderate	High	VIII	6L	0.88 ± 0.08	0.43 ± 0.04	0.32 ± 0.03	0.26 ± 0.00
Specially Designed	High	High	IX	6U	1.43 ± 0.11	0.70 ± 0.05	0.52 ± 0.04	0.43 ± 0.01
Specially Designed	Very High	High	X	7	2.34 ± 0.15	1.14 ± 0.07	0.84 ± 0.06	0.69 ± 0.03

Note: Values of CAV_{DP} are the means and standard deviations taking into account the epistemic uncertainty corresponding to the four databases and the two instrumental intensity measures; $P_{ne}(0.16)_{5U,VII}$ is the nonexceedance probability corresponding to the lower boundary of intensity categories JMA 5U ($I_{JMA} = 5.0$) or EMS/MMI VII ($I_{MM} = 6.5$); all of the data come from Tables 7 and 8.

associated with various values of nonexceedance probability (P_{ne}) and, therefore, whether such a study would be worthwhile.

Table 9 summarizes the mean threshold values of CAV_{DP} and their standard deviations based on the results listed in Tables 7 and 8. The standard deviations represent the epistemic uncertainty corresponding to the four databases (including whether the PSV check is applied) and the two instrumental intensity measures. The levels of earthquake-resistant design that are assigned to the given JMA, MMI, and EMS macroseismic intensity categories and their correspondence to the values of instrumental seismic intensity used to calculate CAV_{DP} are based on our interpretation of the qualitative descriptions of earthquake resistance and damage provided in these intensity scales. Others might interpret these descriptions differently, which is an additional element of epistemic uncertainty not included in the analysis. RC structures described as having no specific earthquake-resistant design in the EMS scale include both engineered and nonengineered construction. Nonengineered structures of this type are typically found in regions of low seismicity where seismic design regulations are nonexistent or are only recommended. They are considered to be similar to buildings of good design and construction as described in the MMI scale and defined by EPRI (1988). The threshold values of CAV_{DP} in the column labeled $P_{ne}(0.16)_{5U,VII}$ correspond to the estimated nonexceedance probabilities that are inferred from the conservative approach used by EPRI (1988, 1991) to establish the original CAV threshold criterion (i.e., 0.35 ± 0.25%). We also give results for less conservative nonexceedance probabilities of 1% and 5%. All of the CAV_{DP} threshold values are found to increase by about 60%–65% with each increase in intensity level.

As indicated in the EPRI Damage Review section, there is a fair amount of conservatism in the EPRI (1991) and USNRC (1997) damage threshold criteria. According to Table 9, the minimum observed values of CAV_{STD} that EPRI found were associated with structural damage correspond to a probability of nonexceedance of over 5% instead of 0.35% and an intensity level that is about one degree higher than that associated with the recommended EPRI criterion. This conservatism would appear to mitigate any lack of consideration of the uncertainty associated with interpreting the damage descriptions in the seismic intensity scales.

Of course, it is up to the USNRC and other nuclear regulatory agencies that might consider adopting the USNRC nuclear power plant shutdown criteria to decide whether the results in Tables 7–9 might warrant further engineering analysis in order to revise these criteria (the first potential use of the prediction equation developed in this study). Therefore, we do not pursue this issue further. However, the results presented in these tables can be used to address the second potential use of the prediction equations developed in this study, that is, to rapidly assess the potential damage to conventional structures after an earthquake. Continuing with the example of a generic RC structure, the EMS scale (Grünthal 1998) indicates that Vulnerability Class C is the most likely vulnerability class for an RC frame or wall without earthquake-resistant design. According to Table 3, damage consistent with Damage Grade 2 (slight structural damage, Table 4) for this vulnerability class begins at EMS (MMI) VII. If one accepts a 5% probability that damage will be less than this given the estimated threshold value of CAV_{DP} for this intensity level, this threshold value is estimated to be approximately 0.3 g-s, according to the summary results listed in Table 9. Following this same logic,

a similar structure would begin to sustain Damage Grade 3 (moderate structural damage, MMI/EMS VIII) at approximately 0.4 g-s, Damage Grade 4 (heavy structural damage, MMI/EMS IX) at approximately 0.7 g-s, and Damage Grade 5 (very heavy structural damage or collapse, MMI/EMS X) at approximately 1.1 g-s. Given these threshold values, a ShakeMap could be produced that would identify those geographic regions where the above levels of damage to generic RC structures without earthquake-resistant design (but of good design and construction) might be expected. Similar assessments could be made for other nonexceedance probabilities, types of structures, and vulnerability classes depending on the intended purpose. One potential purpose of such a map would be to assist in determining where to focus emergency response activities. This would be particularly useful if the potential damage map were overlain on an inventory map of the structures of interest in a manner similar to ShakeCast (e.g., Wald et al. 2006, 2008; Fraser et al. 2008).

A potential issue with using CAV_{DP} to assess and map the damage potential of a general class of structures is the necessity to be able to spatially interpolate the instrumentally derived values. Unlike peak-amplitude and response spectral values, NEHRP site factors (BSSC 2009) cannot be used to spatially interpolate CAV_{DP}, or for that matter any other version of CAV, to other site conditions due in part to their dependence on duration. However, similar site factors for CAV_{DP} can be derived from site terms such as those included in the CAV_{GM} GMPE of Campbell and Bozorgnia (2010b) and imputed to CAV_{DP} through the relationship between $\ln CAV_{DP}$ and $\ln CAV_{GM}$ developed by Campbell and Bozorgnia (2011b). These same two relationships could also be used to estimate CAV_{DP} when no instrumental values are available in the vicinity of a site, similar to the procedure currently used to develop ShakeMaps for peak-amplitude and response spectral values (Wald et al. 1999c).

Based on its correlation with other IMs (Campbell and Bozorgnia 2010a), CAV_{DP} would appear to have a negligible "effect size" (Cohen 1988), a measure of the strength between variables based on the correlation coefficient ρ, when compared to PGV ($\rho = 0.07$) and to PSA with periods in the range $T > 0.4$ s ($\rho < 0.10$), and a small effect size when compared to PGA ($\rho = 0.21$) and to PSA with periods in the range $T \leq 0.4$ s ($0.21 \leq \rho < 0.10$). However, this apparent low correlation is due to the direct relationship between CAV_{DP} and CAV_{GM} and the fact that this latter IM has a large effect size when compared to PGA ($\rho = 0.74$), to PGV ($\rho = 0.69$), and to PSA at periods ranging between 0.01 s ($\rho = 0.74$) and 10 s ($\rho = 0.36$). We further note that, although the correlation coefficient between CAV_{GM} and PSA decreases with period, it remains above 0.5 for periods up to 2 s and has a large effect size even up to a period of 10 s.

SUMMARY AND CONCLUSIONS

We present prediction equations between a variant of the standardized version of CAV, which we refer to as CAV_{DP}, and instrumental measures of JMA seismic intensity (I_{JMA}) and MMI (I_{MM}), both of which have been calibrated to the macroseismic versions of these intensity scales and, therefore, to the qualitative descriptions of structural damage embodied in these scales. CAV_{DP} incorporates in a single parameter all of the ground motion criteria that EPRI used to establish the threshold of damage to conventional buildings of good design and construction and that USNRC conservatively used to establish its nuclear power plant shutdown criteria. We used I_{JMA} and its relationship to the JMA macroseismic intensity

scale and I_{MM} and its relationship to the MMI and EMS macroseismic intensity scales to derive threshold values of CAV_{DP} that correspond to the onset of damage associated with a generic class of RC structures of different degrees of earthquake-resistant design, as inferred from the macroseismic effects described in these intensity scales. Other classes of structures can be evaluated in a similar manner. Our prediction equations can be used to statistically quantify and select an appropriate set of damage threshold criteria for CAV_{DP} that takes into account both aleatory and, to a limited extent, epistemic uncertainty. However, our estimate of epistemic uncertainty does not include the additional uncertainty that corresponds to the association of a specific level of macroseismic intensity with the expected level of structural damage. This is not necessarily an issue considering the demonstrated conservatism in this association based on actual, albeit relatively old, damage data collected by EPRI (1988).

Our analysis estimates that the probability of nonexceedance of the 0.16 g-s EPRI and USNRC threshold criteria, assuming the onset of damage at EMS/MMI VII (JMA 5U), is $0.35 \pm 0.25\%$, depending on the version of the database and instrumental intensity measure that is used in the analysis. Given similarly small nonexceedance probabilities, this conservative threshold criterion increases to 0.26, 0.43, and 0.69 g-s for damage thresholds corresponding to EMS/MMI VIII, IX, and X (JMA 6L, 6U, and 7), respectively, consistent with structures described as having moderate, high, and very high earthquake resistance on the EMS intensity scale. Higher acceptable probabilities of nonexceedance result in even higher values of CAV_{DP}. For example, for a 5% probability of nonexceedance, all of the CAV_{DP} damage threshold values increase by about 65%, consistent with both the increase in CAV_{DP} that corresponds to an increase of one degree of intensity and the conservatism in the CAV_{STD} threshold criteria estimated by EPRI (1988, 1991) from actual damage data.

The relatively strong correlation of CAV_{GM} and, therefore, CAV_{DP} with peak ground motion and response spectral parameters would appear to confirm that CAV-related parameters can represent the response of a broad range of structures, consistent with its strong relationship to seismic intensity. Based on these results, we suggest that CAV_{DP}, or a similar variant of CAV or CAV_{STD}, be considered for use as a single generic damage-related index parameter for rapidly determining the potential degree of damage to structures of various levels of vulnerably or fragility after an earthquake. Such information would be particularly useful in guiding post-earthquake emergency response activities and in rapidly assessing the potential loss to various types of structures. Being a single instrumental intensity measure, it would be amenable to use in ShakeMap (Wald et al. 1999c) and other related ground motion and qualitative damage mapping applications such as a more generic version of ShakeCast (Wald et al. 2006, 2008; Fraser et al. 2008).

Although other ground motion parameters have been found to correlate well with the seismic response of specific types of structures (e.g., Akkar and Özen 2005), other studies have shown that CAV-related parameters are equal to or superior to these other IMs in quantifying the general qualitative earthquake damage inferred from macroseismic effects. These IMs include many peak-amplitude and response spectral parameters as well as duration- and energy-related parameters, including AI. Although AI was found to be almost as good as CAV-related parameters in predicting qualitative estimates of damage in many studies, its prediction is plagued with substantially greater aleatory uncertainty, making it a less

predictable and, therefore, less desirable as a ground motion hazard parameter (Campbell and Bozorgnia 2010b, 2011c).

ACKNOWLEDGEMENTS

This project was partially funded by the International Atomic Energy Agency (IAEA) as part of the activities of Seismic Working Group 1 (WG1) of the Extra Budgetary Program (EBP). Dr. Bozorgnia's participation was partially sponsored by the Pacific Earthquake Engineering Research Center (PEER). Any opinions, findings, and conclusions or recommendations expressed in this material are those of the authors and do not necessarily reflect those of the sponsors. We gratefully acknowledge the constructive comments of Julian Bommer and two anonymous reviewers.

REFERENCES

Abrahamson, N. A., and Youngs, R. R., 1992. A stable algorithm for regression analyses using the random effects model, *Bull. Seismol. Soc. Am.* **82**, 505–510.

Akkar, S., and Özen, Ö., 2005. Effect of peak ground velocity on deformation demands for SDOF systems, *Earthq. Eng. Struct. Dyn.* **34**, 1551–1571.

Aoi, S., Kunugi, T., and Fujiwara, H., 2004. Strong-motion seismograph network operated by NIED: K-Net and KiK-Net, *J. Japan Assoc. Earthq. Eng.* **4**, 65–74.

Arias, A., 1970. A measure of earthquake intensity, in *Seismic Design for Nuclear Power Plants* (Hansen, R. J., ed.), The MIT Press, Cambridge, MA, 438–483.

Atkinson, G. M., and Kaka, S. I., 2007. Relationships between felt intensity and instrumental ground motion, *Bull. Seismol. Soc. Am.* **97**, 497–510.

Atkinson, G. M., and Sonley, E., 2000. Empirical relationships between modified Mercalli intensity and response spectra, *Bull. Seismol. Soc. Am.* **90**, 537–544.

Bozorgnia, Y., Hachem, M. M., and Campbell, K. W., 2010. Ground motion prediction equation ("attenuation relationship") for inelastic response spectra, *Earthquake Spectra* **26**, 1–23.

Building Seismic Safety Council (BSSC), 2009. *NEHRP Recommended Seismic Provisions for New Buildings and Other Structures (FEMA P-750)*, 2009 edition, National Institute of Building Sciences, Washington, D.C.

Cabañas, L., Benito, B., and Herráiz, M., 1997. An approach to the measurement of the potential structural damage of earthquake ground motions, *Earthq. Eng. Struct. Dyn.* **26**, 79–92.

Campbell, K. W., 1986. An empirical estimate of near-source ground motion for a major, $m_b = 6.8$, earthquake in the eastern United States, *Bull. Seismol. Soc. Am.* **76**, 1–17.

Campbell, K. W., and Bozorgnia, Y., 2007. *Campbell-Bozorgnia NGA Ground Motion Relations for the Geometric Mean Horizontal Component of Peak and Spectral Ground Motion Parameters*, PEER 2007/02, Pacific Earthquake Engineering Research Center, University of California, Berkeley.

Campbell, K. W., and Bozorgnia, Y., 2008. NGA ground motion model for the geometric mean horizontal component of PGA, PGV, PGD, and 5% damped linear elastic response spectra for periods ranging from 0.01 to 10 s, *Earthquake Spectra* **24**, 139–171.

Campbell, K. W., and Bozorgnia, Y., 2010a. *Analysis of Cumulative Absolute Velocity (CAV) and JMA Instrumental Seismic Intensity (I_{JMA}) Using the PEER-NGA Strong Motion Database*, PEER 2010/102, Pacific Earthquake Engineering Research Center, University of California, Berkeley.

Campbell, K. W., and Bozorgnia, Y., 2010b. A ground motion prediction equation for the horizontal component of cumulative absolute velocity (CAV) using the PEER-NGA database, *Earthquake Spectra* **26**, 635–650.

Campbell, K. W., and Bozorgnia, Y., 2011a. A ground motion prediction equation for JMA instrumental seismic intensity for shallow crustal earthquakes in active tectonic regimes, *Earthq. Eng. Struct. Dyn.* **40**, 413–427.

Campbell, K. W., and Bozorgnia, Y., 2011b. Predictive equations for the standardized version of cumulative absolute velocity as adapted for use in the shutdown of U.S. nuclear power plants, *Nucl. Eng. Des.* **241**, 2558–2569.

Campbell, K. W., and Bozorgnia, Y., 2011c. A comparison of ground motion prediction equations for Arias intensity and cumulative absolute velocity developed using a consistent database and function form, *Earthquake Spectra*, accepted for publication.

Chiou, B., Darragh, R., Gregor, N., and Silva, W., 2008. NGA project strong-motion database, *Earthquake Spectra* **24**, 23–44.

Cohen, J., 1988. *Statistical Power Analysis for the Behavioral Sciences*, 2nd edition, Lawrence Erbaum Associates, Hillsdale, NJ.

Danciu, L., and Tselentis, G., 2007. Engineering ground-motion parameters attenuation relationships for Greece, *Bull. Seismol. Soc. Am.* **97**, 162–183.

Davenport, P. N., 2003. Instrumental measures of earthquake intensity in New Zealand, Paper 071, *7th Pacific Conference on Earthquake Engineering*, 13–15 February 2003, Christchurch, New Zealand.

Dengler, L. A., and Dewey, J. W., 1998. An intensity survey of households affected by the Northridge, California, earthquake of 17 January 1994, *Bull. Seismol. Soc. Am.* **88**, 441–462.

Dewey, J. W., Reagor, B. G., Dengler, L., and Moley, K., 1995. Intensity distribution and isoseismal maps for the Northridge, California, earthquake of January 17, 1994, *U.S. Geol. Survey Open-File Report 95-92*, Reston, VA.

Earthquake Research Committee, 1998. *Seismic Activity in Japan*, Headquarters for Earthquake Research Promotion, Prime Minister's Office, Government of Japan, Science and Technology Agency, Tokyo.

Ebel, J. E., and Wald, D. J., 2003. Bayesian estimations of peak ground acceleration and 5% damped spectral acceleration from modified Mercalli intensity data, *Earthquake Spectra* **19**, 511–529.

Electrical Power Research Institute (EPRI), 1988. *A Criterion for Determining Exceedance of the Operating Basis Earthquake*, EPRI NP-5930, Palo Alto, CA.

Electrical Power Research Institute (EPRI), 1991. *Standardization of the Cumulative Absolute Velocity*, EPRI TR-100082-T2, Palo Alto, CA.

Electrical Power Research Institute (EPRI), 2006. *Program on Technology Innovation: Use of Cumulative Absolute Velocity (CAV) in Determining Effects of Small Magnitude Earthquakes on Seismic Hazard Analyses*, EPRI 1014099, Palo Alto, CA.

Faenza, L., and Michelini, A., 2010. Regression analysis of MCS intensity and ground motion parameters in Italy and its application in ShakeMap, *Geophys. J. Int.* **180**, 1138–1152.

Fraser, W. A., Wald, D. J., and Lin, K. W., 2008. Using ShakeMaps and ShakeCast to prioritize post-earthquake dam inspections, in *Proc., 4th Geotechnical Earthquake Engineering and Soil Dynamics Conference*, Sacramento, CA, American Society of Civil Engineers Geotechnical Special Publication 181, 1–10.

Grünthal, G. (ed.), 1998. *European Macroseismic Scale 1998*, Cahiers du Centre Européen de Géodynamique et de Séismologie, Conseil de l'Europe, Luxembourg.

Japan Meteorological Agency (JMA), 1996. *On Seismic Intensity*, Gyosei, Tokyo, 46–224 (in Japanese).

Japan Meteorological Agency (JMA), 2011. *Tables Explaining the JMA Seismic Intensity Scale*, http://www.jma.go.jp/jma/en/Activities/inttable.pdf, accessed December 2011.

Kostov, M., 2005. Site-specific estimation of cumulative absolute velocity, in *Proc., 18th International Conference on Structural Mechanics in Reactor Technology (SMiRT 18)*, Beijing, 3041–3050.

Kramer, S. L., and Mitchell, R. A., 2006. Ground motion intensity measures for liquefaction hazard evaluation, *Earthquake Spectra* **22**, 413–438.

Musson, R. M. W., Grünthal, G., and Stucchi, M., 2010. The comparison of macroseismic intensity scales, *J. Seismol.* **14**, 413–428.

Power, M., Chiou, B., Abrahamson, N., Bozorgnia, Y., Shantz, T., and Roblee, C., 2008. An overview of the NGA project, *Earthquake Spectra* **24**, 3–21.

Reed, J. W., and Kassawara, R. P., 1990. A criterion for determining exceedance of the Operating Basis Earthquake, *Nucl. Eng. Des.* **123**, 387–396.

Richter, C. F., 1958. *Elementary Seismology*, W. H. Freeman, San Francisco, CA.

Shabestari, K. T., and Yamazaki, F., 2001. A proposal of instrumental seismic intensity scale compatible with MMI evaluated from three-component acceleration records, *Earthq. Spectra* **17**, 711–723.

Sokolov, V. Y., 2002. Seismic intensity and Fourier acceleration spectra: Revised relationship, *Earthquake Spectra* **18**, 161–187.

Sokolov, V. Y., and Chernov, Y. K., 1998. On the correlation of seismic intensity with Fourier amplitude spectra, *Earthquake Spectra* **14**, 679–694.

Sokolov, V., and Furumura, T., 2008. Comparative analysis of two methods for instrumental intensity estimations using the database accumulated during recent large earthquakes in Japan, *Earthquake Spectra* **24**, 513–532.

Sokolov, V., and Wald, D. J., 2002. Instrumental intensity distribution for the Hector Mine, California, and the Chi-Chi, Taiwan, earthquakes: Comparison of two methods, *Bull. Seismol. Soc. Am.* **92**, 2145–2162.

Trifunac, M. D., and Brady, A. G., 1975. On the correlation of seismic intensity scales with the peaks of recorded strong ground motion, *Bull. Seismol. Soc. Am.* **65**, 139–162.

Tselentis, G. A., and Danciu, L., 2008. Empirical relationships between modified Mercalli intensity and engineering ground-motion parameters in Greece, *Bull. Seismol. Soc. Am.* **98**, 1863–1875.

U.S. Geological Survey (USGS), 2000. *The Severity of an Earthquake*, General Interest Publication, Reston, VA, 15 pp., http://pubs/usgs.gov/gip/earthq4/severitygip.htlm.

U.S. Nuclear Regulatory Commission (USNRC), 1997. *Pre-earthquake Planning and Immediate Nuclear Power Plant Operator Postearthquake Actions*, Regulatory Guide 1.166, Washington, D.C.

Wald, D. J., Dengler, L. A., and Dewey, J. W., 1999a. Utilization of the Internet for rapid community intensity maps, *Seismol. Res. Lett.* **70**, 680–697.

Wald, D. J., Quitoriano, V., Heaton, T. H., and Kanamori, H., 1999b. Relationships between peak ground acceleration, peak ground velocity and modified Mercalli intensity in California, *Earthquake Spectra* **15**, 557–564.

Wald, D. J., Quitoriano, V., Heaton, T. H., Kanamori, H., Serivner, V. W., and Worden, C. B., 1999c. TriNet "ShakeMaps": Rapid generation of instrumental ground motion and intensity maps for earthquakes in southern California, *Earthquake Spectra* **15**, 537–555.

Wald, D. J., Lin, K., Worden, B., and Turner, L., 2006. ShakeCast: Facilitating the use of ShakeMap for post-earthquake decision-making and response within Caltrans and other critical lifeline communities, Paper A22, *5th National Seismic Conference on Bridges & Highways*, 18–20 September 2006, San Mateo, CA, MCEER-06-SP09, Multidisciplinary Center for Earthquake Engineering Research, Buffalo, NY.

Wald, D., Lin, K. W., and Porter, K., 2008. ShakeCast: Automating and improving the use of ShakeMap for post-earthquake decision-making and response, *Earthquake Spectra* **24**, 533–553.

Wood, H. O., and Neumann, F., 1931. Modified Mercalli intensity scale of 1931, *Bull. Seismol. Soc. Am.* **21**, 277–283.

(Received 27 September 2010; accepted 11 June 2011)